Polymer Degradation and Stability 105 (2014) 248–256

Contents lists available at ScienceDirect

Polymer Degradation and Stability

journal homepage: www.elsevier.com/locate/polydegstab

Comparative study on the flame retarded efficiency of melamine phosphate, melamine phosphite and melamine hypophosphite on poly(butylene succinate) composites

Hongyu Yang [a,b,c], Lei Song [a,**], Qilong Tai [a], Xin Wang [a], Bin Yu [a,b,c], Yao Yuan [a], Yuan Hu [a,c,*], Richard K.K. Yuen [b]

[a] State Key Laboratory of Fire Science, University of Science and Technology of China, 96 Jinzhai Road, Hefei, Anhui 230026, PR China
[b] Department of Building and Construction, City University of Hong Kong, Tat Chee Avenue, Kowloon, Hong Kong
[c] USTC-CityU Joint Advanced Research Centre, Suzhou Key Laboratory of Urban, Public Safety, Suzhou Institute for Advanced Study, University of Science and Technology of China, 166 Ren'ai Road, Suzhou, Jiangsu 215123, PR China

ARTICLE INFO

Article history:
Received 11 February 2014
Received in revised form
10 April 2014
Accepted 25 April 2014
Available online 5 May 2014

Keywords:
Phosphorus-containing melamine salts
Phosphorus valency
Poly(butylene succinate)
Flame retarded efficiency
Flame-retardant mechanism

ABSTRACT

The main aim of this work was to investigate the flame retarded efficiency of melamine phosphate (MP), melamine phosphite (MPi) and melamine hypophosphite (MHP) on poly(butylene succinate) (PBS) composites. The flame retardant, thermal degradation and combustion properties of PBS composites were characterized by limiting oxygen index (LOI) test, vertical burning (UL-94) test, thermogravimetric analysis (TGA) and cone calorimeter (Cone), respectively. The LOI results showed that the LOI values followed the sequence of PBS/MP < PBS/MHP < PBS/MPi at the same additive loadings. TGA results indicated that the initial decomposition temperature of PBS composites decreased with the decrease of phosphorus valence state and the incorporation of all three compounds could promote the char formation. Adding these three compounds into PBS matrix can decrease the peak heat release rate (PHRR) obviously from cone calorimeter results. Scanning electron microscopy (SEM) was employed to characterize the morphology and structure of the char residues. The flame-retardant mechanism in gaseous phase and condensed phase were investigated by thermogravimetric analysis/infrared spectrometry (TG-IR) and in situ Fourier transform infrared spectroscopy (in situ FTIR), respectively, and the possible flame-retardant mechanism was proposed.

1. Introduction

Phosphorus-containing flame retardants as a species of halogen-free flame retardants have been widely used to impart polymer composites with flame retardancy due to their high efficiency. According to previous literature [1–8], many kinds of phosphorus-containing flame retardants have been investigated, such as red phosphorus (Pr), hypophosphites, phosphites, phosphates, etc. These compounds function in gaseous phase, condensed phase or both. In the gaseous phase [9,10], some phosphorus-containing compounds play a role in flame inhibition through radical trapping; in the condensed phase [11,12], they promote the formation of carbon char or inorganic residue and then acts as a barrier, which decreases the mass loss rate and heat release. In general, the phosphorus-containing compounds (act as acid source) are combined with carbon source (or char forming agent) and gas source (or blowing agent) to form an intumescent flame retardant system [13]. Because of the formation of intumescent compact char layer during combustion, which can effectively protect the polymer matrix, the intumescent system exhibits high flame retardant efficiency.

Recently, hypophosphites such as aluminum hypophosphite (AHP), rare earth hypophosphite (REHP) have been used as effective flame retardant for poly (1,4-butylene terephthalate) (PBT) [14], Polyamide (PA) [15], Polylactide (PLA) [16], etc. Phosphites, such as trimethyl phosphite is a good flame retardant additive used in the electrolyte [17]. Phosphates [18–20], including ammonium polyphosphate (APP), melamine phosphate (MP), melamine polyphosphate (MPP), etc. are the most common flame retardants on the market. However, the flame-retardant mechanisms of these

* Corresponding author. State Key Laboratory of Fire Science, University of Science and Technology of China, 96 Jinzhai Road, Hefei, Anhui 230026, PR China. Tel./fax: +86 551 3601664.
** Corresponding author. Tel.: +86 551 63600081.
E-mail addresses: leisong@ustc.edu.cn (L. Song), yuanhu@ustc.edu.cn (Y. Hu).

http://dx.doi.org/10.1016/j.polymdegradstab.2014.04.021
0141-3910/

compounds above are not the same. Some compounds mainly function in condensed phase, while others mainly act in gaseous phase. The largest difference among these compounds is the phosphorus valency.

Therefore, to explore the flame-retardant mechanism of several typical phosphorus flame retardants with varied valence state of phosphorus on improving the fire retardancy of polymer materials is necessary and important. Braun et al. [21]. systemically investigated the influence of the oxidation state of phosphorus on the decomposition and fire behavior of flame-retarded epoxy resin composites by using different hardeners such as phosphine oxide, phosphinate, phosphonate and phosphate-based ones. Modesti et al. [22]. reported decomposition/pyrolysis studies of polyurethane (PU) rigid foams containing phosphinate, phosphonate or phosphate as flame retardant. Wilkie et al. [23] studied the influence of oxidation state of phosphorus on the thermal and flammability of polyurea and epoxy resin. Since deep understanding of the actual mechanisms is rather in its infancy, further systemically studying the structure property relationships of phosphorus-containing compounds on other polymers like polyester, polyolefin, etc. is required.

As a kind of biodegradable aliphatic polyesters, poly(butylene succinate) (PBS) has been widely used in many fields (such as agricultural films, packing materials, injection-molded products). Be conscious of the inherent flammability of PBS which severely restricted its potential applications, Chen et al. [24] and Wang [25] recently researched the intumescent flame retardant poly(butylene succinate) using ammonium polyphosphate as acid source, melamine as source gas, fumed silica and graphene as synergistic agent, respectively. Notable intumescent char can be observed in the optimal proportion of their LOI results, indicating that PBS itself can serve as carbon source in intumescent flame retardant PBS composite system.

In this work, three simple salts with different phosphorus valency including melamine hypophosphite (MHP), melamine phosphite (MPi) and melamine phosphate (MP) were prepared and blended with poly(butylene succinate) (PBS) to obtain a series of flame retardant PBS composites. The flammability and thermal properties of flame retardant PBS composites were evaluated by limiting oxygen index test, UL-94, cone calorimeter (Cone), and thermogravimetric analysis (TGA). In order to further understand their flame-retardant mechanism, selective samples have been studied by thermogravimetric analysis-infrared spectrometry (TG-IR) technique and in situ Fourier transform infrared spectroscopy (in situ FTIR).

2. Experimental section

2.1. Materials

Poly(butylene succinate) (PBS, weight-average molecular weight: 170,000, hydroxyl end-capped) was purchased from Anqing Hexing Chemicals Co. Ltd. (Anhui, China). Melamine (CP), phosphoric acid (AR, ≥85%), phosphorous acid (AR, ≥99%) and hypophosphorous acid (GR, 50% aqueous solution) were purchased from Sinopharm Chemical Reagent Co. (Shanghai, China).

2.2. Synthesis of melamine phosphate (MP), melamine phosphite (MPi) and melamine hypophosphite (MHP)

In typical experiment, 37.84 g (0.3 mol) melamine was dissolved in 750 ml deionized water in a 1000 ml three-necked, round-bottomed flask fitted with a mechanical stirrer, flux condenser and dropping funnel, and stirred at 95 °C for 30 min. 34.6 g (0.3 mol) phosphoric acid was added dropwise to the above reaction flask and then kept at 95 °C for 1 h. After cooling to room temperature, the precipitate was filtered, washed with cold water and then dried to a constant weight. The obtained white solid was melamine phosphate (MP). For MPi, 37.84 g (0.3 mol) melamine was dissolved in 750 ml deionized water in a 1000 ml three-necked, round-bottomed flask fitted with a mechanical stirrer, flux condenser and dropping funnel, and stirred at 95 °C for 30 min. 24.8 g (0.3 mol) phosphorous acid which dissolved in 50 ml deionized water was added dropwise to the above reaction flask and then kept at 95 °C for 1 h. After cooling to room temperature, the precipitate was filtered, washed with cold water and then dried to a constant weight. The synthesis of MHP was similar to that of MPi. In this procedure, to react with 0.3 mol melamine, 39.6 g (0.3 mol) hypophosphorous acid (50% aqueous solution) was added. All of these three compounds are white powder as can be seen from digital images in Fig. 1.

2.3. Preparation of the PBS samples

All samples were prepared on a two-roll mill at a temperature range of 120–125 °C for 15 min. After mixing, the samples were hot-pressed under 10 MPa for 10 min at about 125 °C into sheets of suitable thickness and size for analysis. The composition of the PBS composites is listed in Table 1.

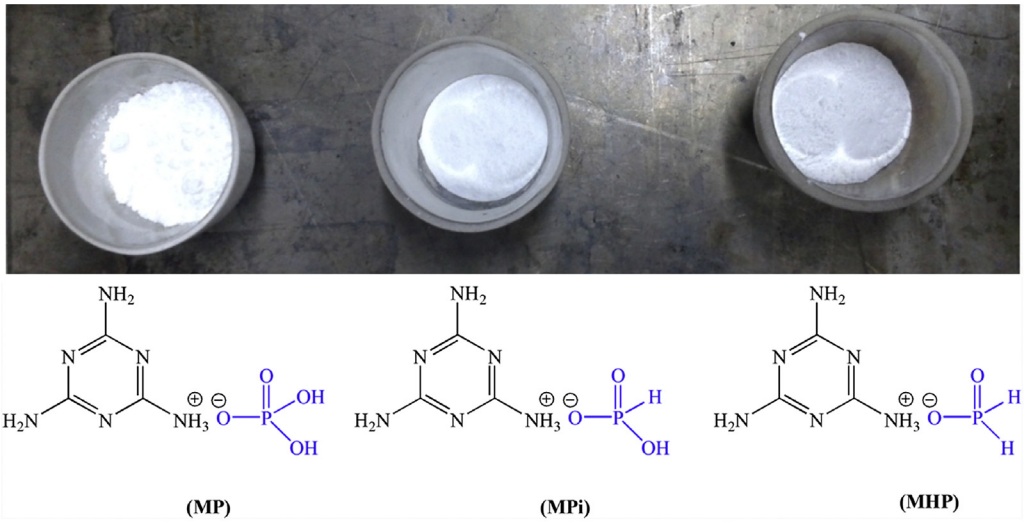

Fig. 1. The digital images and chemical structure of MP, MPi and MHP.

Table 1
LOI and UL-94 results of PBS samples.

Sample	PBS	MP	MPi	MHP	LOI (%)	UL-94[a]			
						t_1/t_2[b]	Dripping	Rating	Ignite the absorbent cotton
PBS-0	100	0	0	0	21	–[c]	Yes	NR[d]	Yes
PBS-1	90	10	0	0	23.5	5.6/2.3	Yes	V-2	Yes
PBS-2	80	20	0	0	26	1.2/9.5	No/yes[e]	V-2	Yes
PBS-3	70	30	0	0	28	0.8/1.6	No	V-0	No
PBS-4	90	0	10	0	24.5	8.9/1.5	No/yes	V-2	Yes
PBS-5	80	0	20	0	29	0.9/8.5	No/yes	V-2	Yes
PBS-6	70	0	30	0	30.5	0.9/1.4	No	V-0	No
PBS-7	90	0	0	10	24	0.8/2.2	No/yes	V-2	Yes
PBS-8	80	0	0	20	28	0.8/0.9	No/yes	V-2	Yes
PBS-9	70	0	0	30	29	0.8/1.5	No	V-0	No

[a] The thickness of PBS samples is 3 mm.
[b] t_1, t_2 represent the after flame time after the first and second 10 s flame application, respectively.
[c] Means that the specimen burns completely and therefore t_1, t_2 is not detectable.
[d] NR represents no rating.
[e] No/yes corresponds to the first/second flame application.

2.4. Characterization

Fourier transform infrared (FTIR) spectroscopy was obtained at 4 cm^{-1} resolution and averages of spectra were obtained from at least 16 scans in the standard wavenumber range of 400–4000 cm^{-1} by Nicolet 6700 spectrometer (Nicolet Instrument Company, USA) using KBr pellets.

^{31}P NMR measurements were performed on AVANCE 400 Bruker spectrometer using dimethyl sulfoxide-d6 as solvent.

The limiting oxygen index (LOI) test was measured according to ASTM D2863. The apparatus used was an HC-2 oxygen index meter (Jiangning Analysis Instrument Company, China). The specimens used for the test were of dimensions 100 mm × 6.5 mm × 3 mm.

The vertical test was carried out on a CFZ-2-typeinstrument (Jiangning Analysis Instrument Company, China) according to the UL 94 test standard. The specimens used were of dimensions 130 mm × 13 mm × 3 mm.

The cone calorimeter (FTT, UK) tests were performed according to ISO 5660 standard procedures. Each specimen of dimensions 100 mm × 100 mm × 3 mm was wrapped in aluminum foil and exposed horizontally to an external heat flux of 35 kW/m^2.

TG experiments were performed using a Q5000 IR thermoanalyzer instrument under air atmosphere. The specimens (about 5–10 mg) were heated from room temperature to 700 °C at a linear heating rate of 20 °C/min.

Thermogravimetric analysis/infrared spectrometry (TG-IR) was performed using the TGA Q5000 IR thermogravimetric analyzer that was interfaced to the Nicolet 6700 FT-IR spectrophotometer. About 5.0 mg of the sample was put in an alumina crucible and heated from 30 to 700 °C. The heating rate was set as 20 °C/min (nitrogen atmosphere).

The in situ FTIR spectra were recorded in the range of room temperature (RT) to 550 °C at 10 °C/min (air atmosphere) on a MAGNA-IR 750 spectrometer (Nicolet Instrument Company, USA).

Scanning electron microscopy (SEM) was performed on the cross-sections of the samples using a Hitachi X650 scanning electron microscope. The slices were adhibitted on the copper plate and then coated with a conductive layer of gold before the measurement.

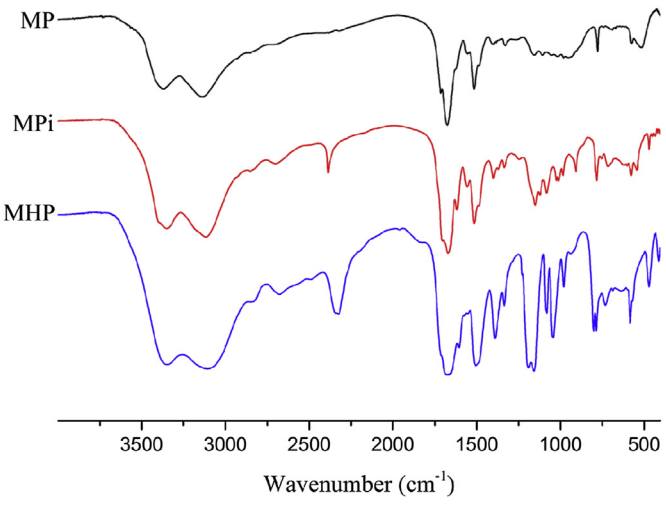

Fig. 2. FTIR spectrum of MP, MPi and MHP.

3. Results and discussion

3.1. Characterization of MP, MPi and MHP

The infrared spectra of MP, MPi and MHP are shown in Fig. 2. For MP, the absorptions at 3371, 3129 and 1676 cm^{-1} are assigned to the asymmetric stretching vibration, symmetric stretching vibration and deformation vibration of NH_2, respectively [26]. The bands at 1332 cm^{-1} are assigned to stretching vibration of P]O [27]. The peaks at 1404 and 983 cm^{-1} are attributed to P–OH absorptions. The out of place absorption of triazine rings appears at 781 cm^{-1}. Different from MP, a new peak at 2386 cm^{-1} appears in the spectra of MPi, which is assigned to stretching vibration of P–H [28]. Other absorption peaks are similar to those of MP. For MHP, a strong absorption peak around 2324 cm^{-1} which correspond to the stretching vibration of P–H. The relative intensity of the peak is higher than that of MPi due to the abundant P–H bands in MHP. Other absorptions of $-NH_2$, P–OH, and P]O can also be found in the spectra. The chemical structures of MP, MPi and MHP were further confirmed by the ^{31}P NMR. As can be seen in Fig. 3, only a sing peak at 0, 0.86 and 1.34 ppm was found for MP, MPi and MHP, respectively. The above results basically confirm the structure of these three compounds as shown in Fig. 1.

3.2. Flame retardant properties

The flame retardant properties of pure PBS and flame retardant PBS composites were examined by LOI and UL-94 tests, as

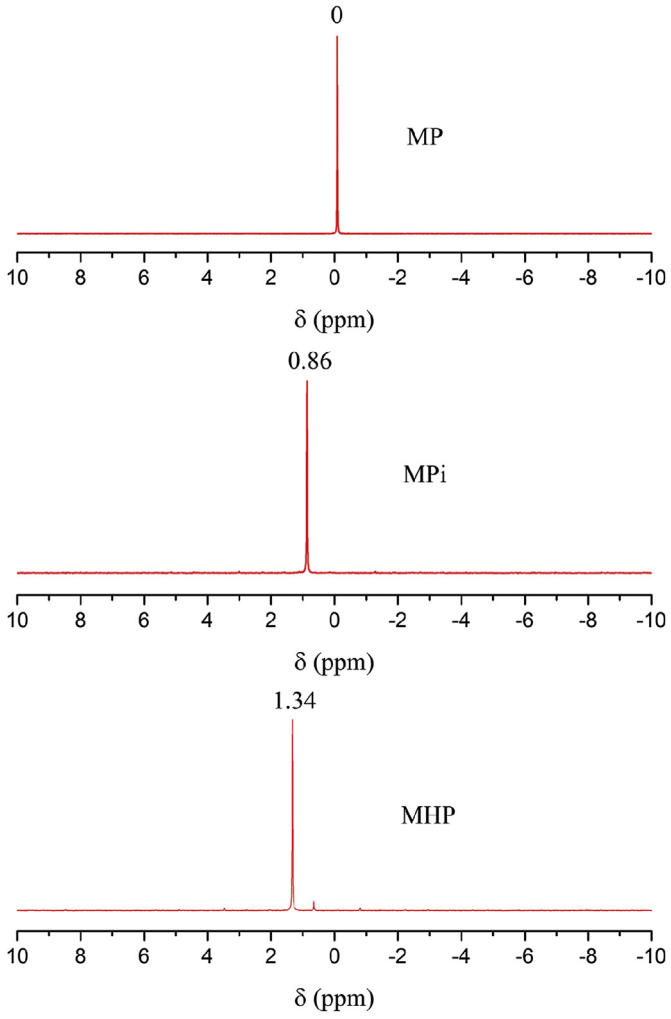

Fig. 3. The ^{31}P NMR spectrum of MP, MPi and MHP.

presented in Table 1 and Fig. 4. It can be found that the LOI value of neat PBS is 21% and no rating in the UL-94 test. With the increase of MP, MPi or MHP content, the LOI values of each PBS hybrids increase gradually. However, the increments on the LOI values of each sample at the same loadings are not the same, indicating the different flame retardant efficiency of these three phosphorus-containing compounds. Meanwhile, the LOI values of each sample at the same loadings show the following rule: MPi/PBS > MHP/PBS > MP/PBS. From the UL-94 results, when the flame retardant loading was 10 wt%, all of the three samples can achieve V-2 rating. PBS-1, which containing 10 wt% MP displays dripping behavior during both of the first and second flame application. While dripping behavior only occurs in the second flame application of PBS-4 (PBS/10 wt% MPi) and PBS-7 (PBS/10 wt% MHP). The samples containing 20 wt% flame retardants also can only pass V-2 rating, because all of the three samples exhibit dripping behavior in the second flame application and it can ignite the absorbent cotton. When the flame retardant loadings further increase to 30 wt%, all of them can achieve V-0 rating. In addition, another special phenomenon that MHP/PBS composites exhibit short extinction time at the UL-94 test indicates the strong self-extinguishing property. The results indicate that the flame retardant properties of MP, MPi and MHP in PBS matrix are different. The retardant mechanism of each compound should be further researched.

Cone calorimeter [29], a small-scale test, has been widely used to predict the flammability behavior of materials in real fire

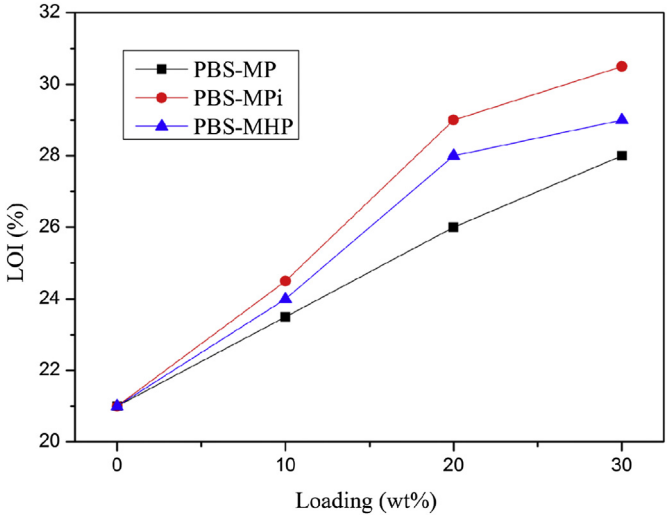

Fig. 4. Effect of MP, MPi and MHP on the LOI results of the PBS composites.

scenarios due to that some of its results possess good correlation with those obtained from large-scale fire tests. From cone calorimeter, several key parameters such as heat release rate (HRR), total heat release (THR), peak HRR (PHRR), time to ignition (TTI) and time to peak HRR can be obtained, which could be employed to evaluate the developing, spreading, and intensity of fires.

Heat release rate (HRR) and total heat release (THR) results of PBS samples are shown in Figs. 5, 6, respectively. The control sample burn very fast after ignition and appears as a sharp peak (PHRR = 613 kW/m^2) on the HRR curve. Incorporating all of the three compounds into PBS matrix can decrease the PHRR obviously. However, the decrements and the curve shape of each sample are not the same. Both of PBS/MP and PBS/MHP composites show ignition in advance except PBS/MPi. For the PBS/MP composites, the PHRR value is 413 kW/m^2 and 32.6% lower than that of pure PBS. It can be observed from Fig. 5 that two peaks appear in the curve of PBS/MP samples. The higher peak appearing around 110s is due to the heat release of combustible gas produced by the pyrolysis of PBS, but the peak value quickly reduces due to the formation of intumescent carbonaceous layer. The lower peak appearing around 200s is attributed to the partial breakage of the char layer from

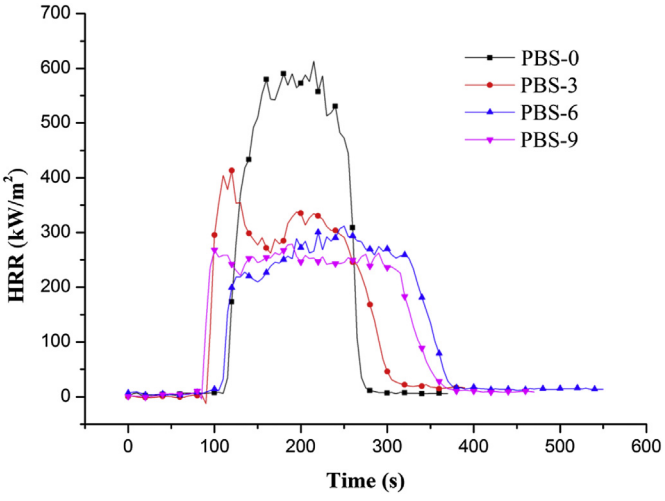

Fig. 5. HRR curves of pure PBS, PBS/MP, PBS/MPi, and PBS/MHP composites.

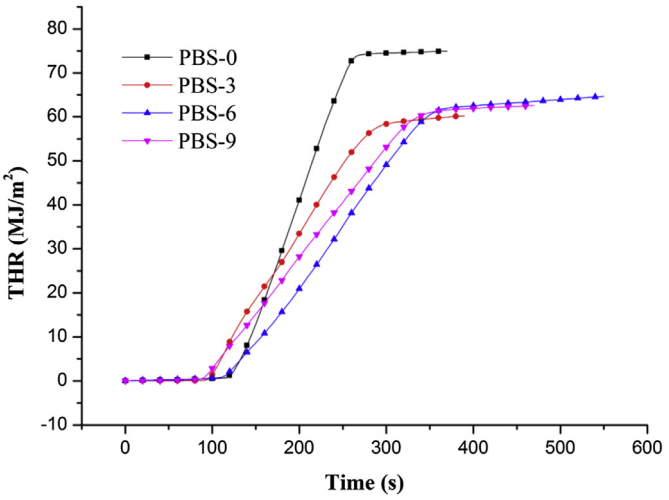

Fig. 6. THR curves of pure PBS, PBS/MP, PBS/MPi, and PBS/MHP composites.

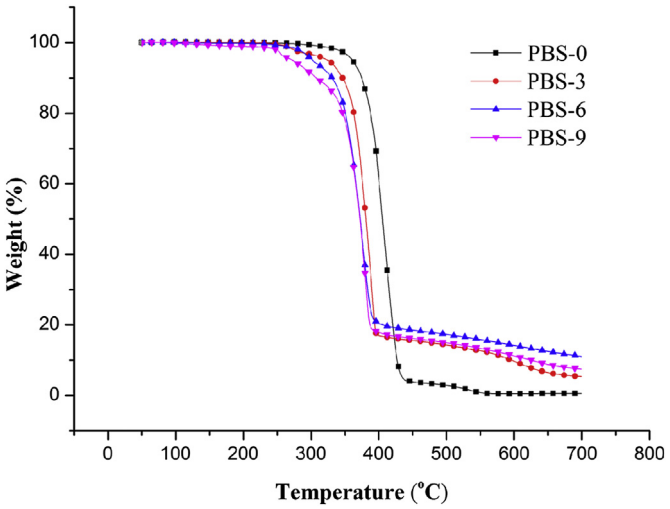

Fig. 7. TG curves of pure PBS, PBS/MP, PBS/MPi, and PBS/MHP composites in air atmosphere.

continuous high-temperature oxidation. For PBS/MPi and PBS/MHP, the initial heat release is controlled at a low level and the PHRR value of PBS/MPi and PBS/MHP were 312 and 279 kW/m^2, respectively, indicating their high suppressive efficiency of heat release. However, the decrements of total heat release (THR) are not very remarkable because of the prolonged burning time as can be seen from the broad peak width in the PHRR curves.

The fire performance index (FPI), which is used to evaluate the fire safety performance of materials, is obtained as the proportion of TTI and PHRR. The higher of the FPI value, the higher safety performance of the materials. High FPI values indicate high TTI or low PHRR. High TTI means more valuable time to evacuate and low PHRR slow down the growth of the fire. The FPI values are presented in Table 2. All of the PBS samples with additives possess higher FPI values than that of control sample. Among them, the FPI value of PBS/MPi is the highest, followed by PBS/MHP and PBS/MP.

The average mass loss rate (AMLR) and the char yield (CY) of flame retardant filled composites are obviously reduced and increased respectively compared with the pure PBS. These phenomena can be attributed to the incomplete combustion of PBS in the presence of phosphorus-containing compounds, and these compounds undergo the carbonization process during combustion.

3.3. Thermal properties

Fig. 7 shows thermogravimetric (TG) curves of pure PBS, PBS/MP, PBS/MPi, and PBS/MHP. The temperature of 5% weight loss ($T_{d,-5\%}$) (onset decomposition temperature), temperature of maximum rate of weight loss (T_{max}) and char residue at 700 °C are listed in Table 3 to evaluate the thermal stability of the samples. It can be seen clearly that each PBS composites filled with these three compounds present lower initial decomposing temperature and higher char yield compared with those of pure PBS. Moreover, the initial decomposing temperature of PBS samples decreases with the decrease of phosphorous valence, indicating that the compound with low phosphorous valence is more unstable during the heating process. However, the char residue of samples gradually enhances according to the following rule: pure PBS < PBS/MP < PBS/MHP < PBS/MPi, which is different with the change rule of phosphorous valence, indicating the complicated char-forming mechanism among these compounds. The detailed mechanism would be analyzed by TG-IR and in situ FTIR to understand the chemical changes in gaseous phase and condensed phase during the thermal degradation process.

Table 2
Cone calorimeter data for PBS, PBS/MP, PBS/MPi and PBS/MHP composites[a] at 35 kW m^{-2} heat flux.

Samples	TTI(s)	t_p(s)	PHRR (kW/m^2)	THR (MJ/m^2)	FPI (10^{-2})	AMLR (10^{-2} g/s/m^2)	CY (%)
PBS-0	108	215	613	74.9	17.6	16.9	6.6
PBS-3	86	120	413	58.3	20.8	14.1	22.3
PBS-6	105	250	312	64	33.7	6.6	21.3
PBS-9	81	190	279	60.9	29	10.9	21

[a] TTI: time to ignition, ±2 s; t_p: time to reach the peak HRR, ±2 s; PHRR: peak heat release rate, ±15 kW/m^2; THR: total heat release, ±0.5 MJ/m^2; FPI: fire performance index, is defined as the proportion of TTI and PHRR; AMLR: average mass loss rate, ±0.1 g/s/m^2; CY: char yield, ±0.5%.

3.4. TG-IR characterization of volatile products

In order to further understand the flame-retardant mechanism of these three compounds in gaseous phase. TG-IR technique [30] was used to analyze the gases evolved during the thermal decomposition of MP, MPi and MHP. The TG-IR results are presented in Fig. 8. As shown in Fig. 8 (a), it could be found that the absorbance of total pyrolysis products of these three compounds is quite different. MP is stable until the absorbance increases rapidly around 16 min. The FTIR spectra of gaseous products from MP at selected time (temperature) are shown in Fig. 8 (b). The typical absorption peaks of PBS composites appear at 3735, 3626, 3331, 2360, 2309, 1626, 1075, 968, 931 and 669 cm^{-1}. Among them, peaks at 3735, 3626 and 1075 cm^{-1} are due to H_2O absorptions; peaks appearing at 2360, 2309 and 669 cm^{-1} are ascribed to absorptions of CO_2, meanwhile peaks appearing at 3331, 1626, 968, and 931 cm^{-1} are attributed to absorptions of gaseous ammonia [27,31].

Table 3
TG data of pure PBS, PBS/MP, PBS/MPi, and PBS/MHP composites in air atmosphere.

Samples	$T_{d,-5\%}$ (°C)	T_{max} (°C)	Char residue at 700 °C ± 0.5 (%)
PBS-0	361	402	0.6
PBS-3	324	390	5.4
PBS-6	302	377	11.1
PBS-9	272	380	7.5

All of these three compounds (H_2O, CO_2 and NH_3) coming from the decomposition of MP are non-flammable gases, which can dilute the combustible gas in gas phase. Compared with MP, MPi is slightly less stable in the initial stage of decomposition since the infrared absorption appears earlier than that of MP as can be seen in Fig. 8 (a). However, it can be clearly observed that a new peak (2320 cm^{-1}) appears around 16 min (365 °C) in Fig. 8 (c), which can be attributed to the absorptions of PH_3 [22]. Moreover, PH_3 generation occurs in the main thermal decomposition temperature range of PBS (350–450 °C), which may plays an important role in flame retardancy of PBS. The absorptions of CO_2, NH_3 and H_2O can also be detected during the decomposition of MPi from the IR spectra. MHP is the most unstable compound comparing with MP and MPi. From Fig. 8 (a), the IR absorptions appear after 5 min. Around 200–280 °C, the absorption of PH_3 at 2320 cm^{-1} can be detected, indicating that PH_3 can also generate in the decomposition of MHP. However, the premature large release of PH_3 before the decomposition of PBS is not desirable for endowing good flame retardant effect to PBS matrix. This result could be used to explain the lower flame retardant efficiency of PBS/MHP compared with that of PBS/MPi in LOI results. The obvious absorptions of CO_2 (2360, 2309 cm^{-1}), NH_3 (968, 933 cm^{-1}) also appear after 12 min (280 °C) from the pyrolysis of MHP. From the detailed analysis above, all of these three compounds can release non-flammable gases such as CO_2, NH_3, H_2O, etc. which are beneficial to diluting combustible gases generated from pyrolysis of PBS. Both MPi and MHP can generate PH_3. The MPi performs the best flame retardant effect among these three flame retardants due to the release time of PH_3 from MPi well matching with that of PBS decomposition. However, the premature release of PH_3 during the MHP decomposition is of no benefit to the improvement of fire resistance of PBS composites.

3.5. In situ FTIR analysis

In order to investigate the influence of MP, MPi and MHP on thermal oxidative degradation process of PBS, in situ FTIR was utilized to monitor the chemical structure changes in the condensed phase of each sample on heating in air.

The FTIR spectra of each sample at different degradation temperatures are shown in Fig. 9. It can be seen from Fig. 9 (a) that the characteristic absorption bands of pure PBS appear at 2950 cm^{-1} (C–H stretching vibration of $-CH_2-$), 1720 cm^{-1} (C]O stretching vibration), 1157 cm^{-1} (stretching vibration of C–O band), 1043 cm^{-1} and 955 cm^{-1} (associated with the crystallization of PBS) [32]. The peak shift from 1720 cm^{-1} to 1741 cm^{-1} with the increase of temperature is due to partial dissociation of hydrogen-bond-associated C]O bonds [24]. The relative intensities of characteristic peaks of PBS do not change below 300 °C except for the absorption at 1043 cm^{-1} and 955 cm^{-1}, indicating the crystal change on the heating process. When the temperature rise up to 350 °C, the intensities of peaks at 2950, 1720, 1157, and 1043 cm^{-1}

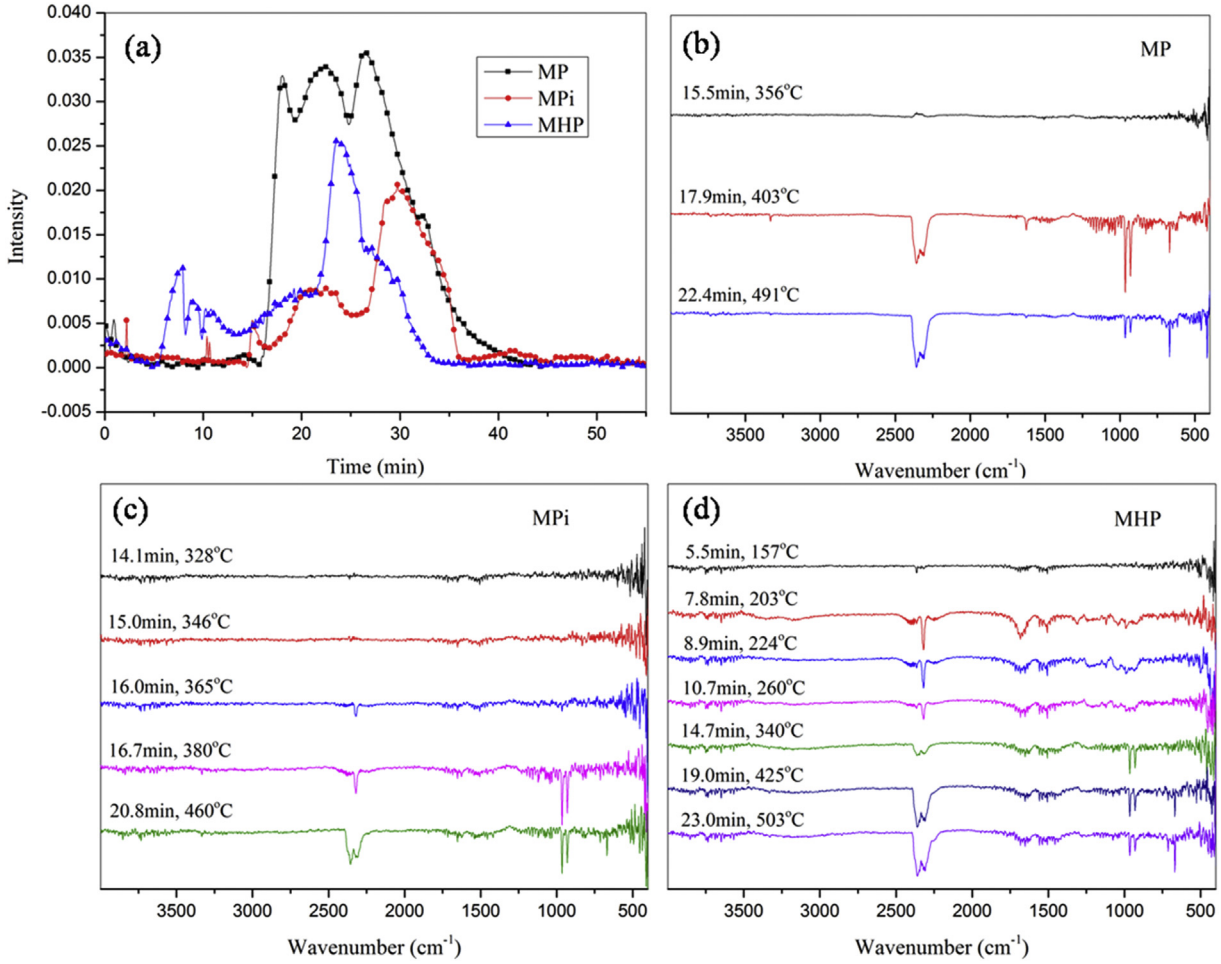

Fig. 8. Absorbance of total pyrolysis products of MP, MPi and MHP (a); FTIR spectra of pyrolysis products from MP (b), MPi (c) and MHP (d) at different time and temperature (in nitrogen atmosphere).

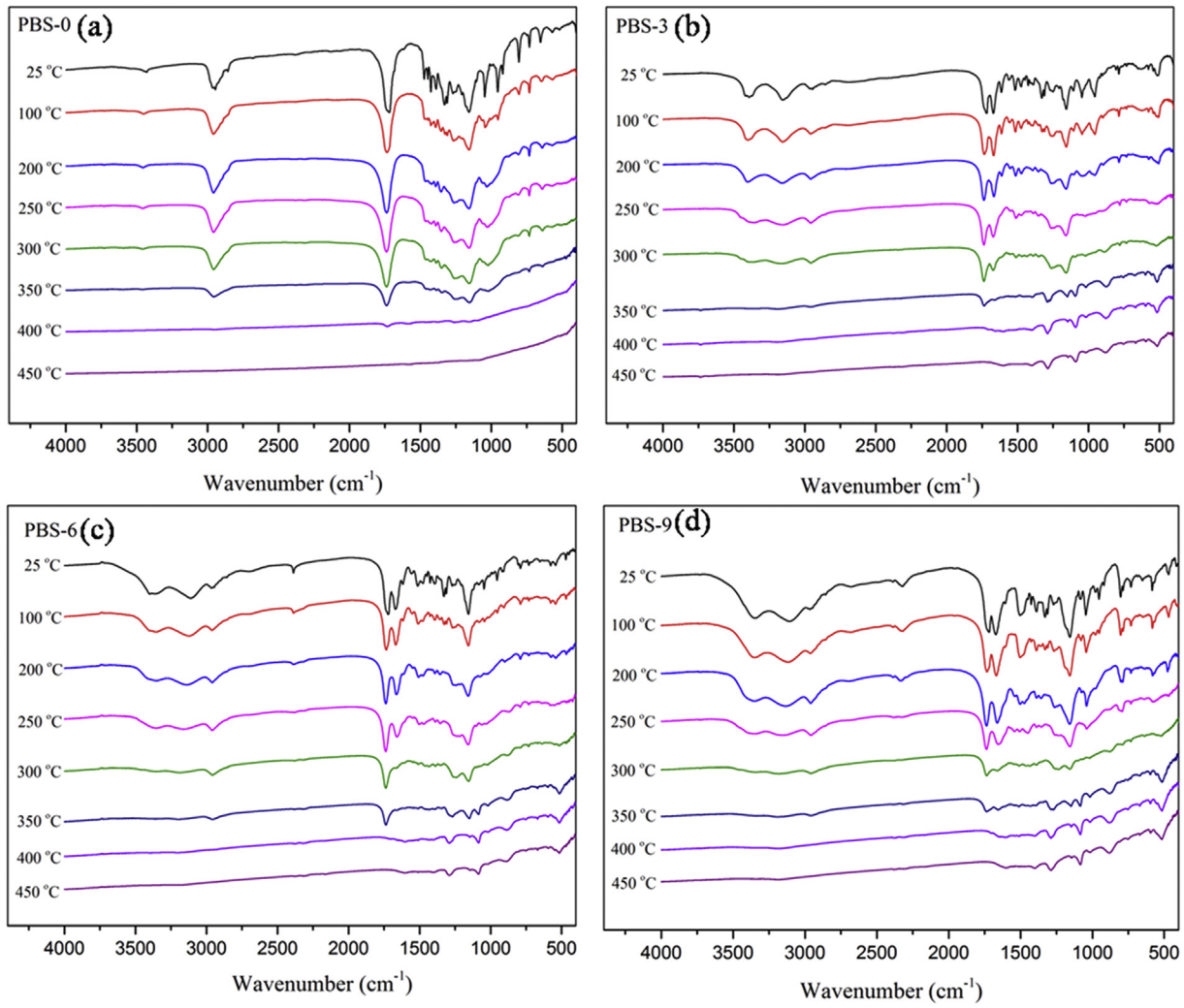

Fig. 9. In situ FTIR spectra for the degradation process of pure PBS (a), PBS/MP (b), PBS/MPi (c) and PBS/MHP (d) at different temperatures (in air atmosphere).

decrease simultaneously, indicating that depolymerization of PBS occurs. At 400 °C, most of bands nearly disappear, indicating that PBS decomposes completely.

The FTIR spectra of PBS/MP at different temperatures are shown in Fig. 9 (b). Compared with pure PBS, the new peaks at 3360–3420 cm^{-1} are corresponding to the overlapping peaks of P–OH absorptions and asymmetric stretching vibration of NH_2. Absorption peaks at 3160 and 1670 cm^{-1} are corresponding to symmetric stretching vibration and deformation vibration of NH_2, respectively, which are derived from the IR absorption of MP. From room temperature to 300 °C, the main absorption peaks of PBS/MP exhibit little change. However, when the temperature increases to 350 °C, the characteristic absorption peaks of NH_2 at 3360, 3160 and 1670 cm^{-1} decrease sharply, indicating the rapid releases of NH_3 from the decomposition of MP. The absorption of methylene at 2950 cm^{-1} almost disappears completely, which is attributed to the depolymerization of PBS, indicating that the presence of MP catalyzes the degradation of PBS matrix. The C]O absorption at 1738 cm^{-1} and the C–O band at 1157 cm^{-1}disappear as well at 400 °C, whereas some of absorption peaks at 1400, 1290, 1145, 1090, 880 cm^{-1} still exist. The peaks at 1400 and 1290 cm^{-1} can be ascribed to the absorption of phosphorousoxynitrides [26] and P]O (in phosphate ester), respectively. The peak at 1145 cm^{-1} is assigned to the absorption of pyrophosphates and/or polyphosphates [26]. The peaks of 1090 and 880 cm^{-1} are due to the symmetric and asymmetric stretching vibration of P–O–P groups [25]. The presence of MP catalyzes the degradation of PBS and promotes the formation of stable char, which can protect the inner PBS matrix from further degradation during combustion.

The FTIR spectra of PBS/MPi and PBS/MHP at different temperatures are shown in Fig. 9 (c) and (d), respectively. General absorption peaks of both PBS/MPi and PBS/MHP are similar to that of PBS/MP except for the absorptions at 2319-2391 cm^{-1}, which are due to the P–H band in MPi and MHP. The intensity of P–H stretching vibration of both MPi and MHP decreases with the increase of temperature from room temperature to 200 °C, and then disappears at 250 °C, which is attributed to the main oxidation degradation of MPi and MHP occurring in this temperature range. The disappearance of P–H band is due to the release of PH_3 and formation of orthophosphate. The existence of P]O, P–O–C and P–O–P bands at 1290, 1145, 1090 and 880 cm^{-1} in residue of both PBS/MPi and PBS/MHP, indicating that MPi and MHP also possess flame retardant effect in condensed phase.

3.6. Investigation on the char formation

Fig. 10 shows the SEM micrographs for the char residues of PBS/MP, PBS/MPi and PBS/MHP after cone calorimeter test. It can be seen visibly that the SEM images of these three samples are quite different. The residue of PBS/MP is sturdy whereas some big holes

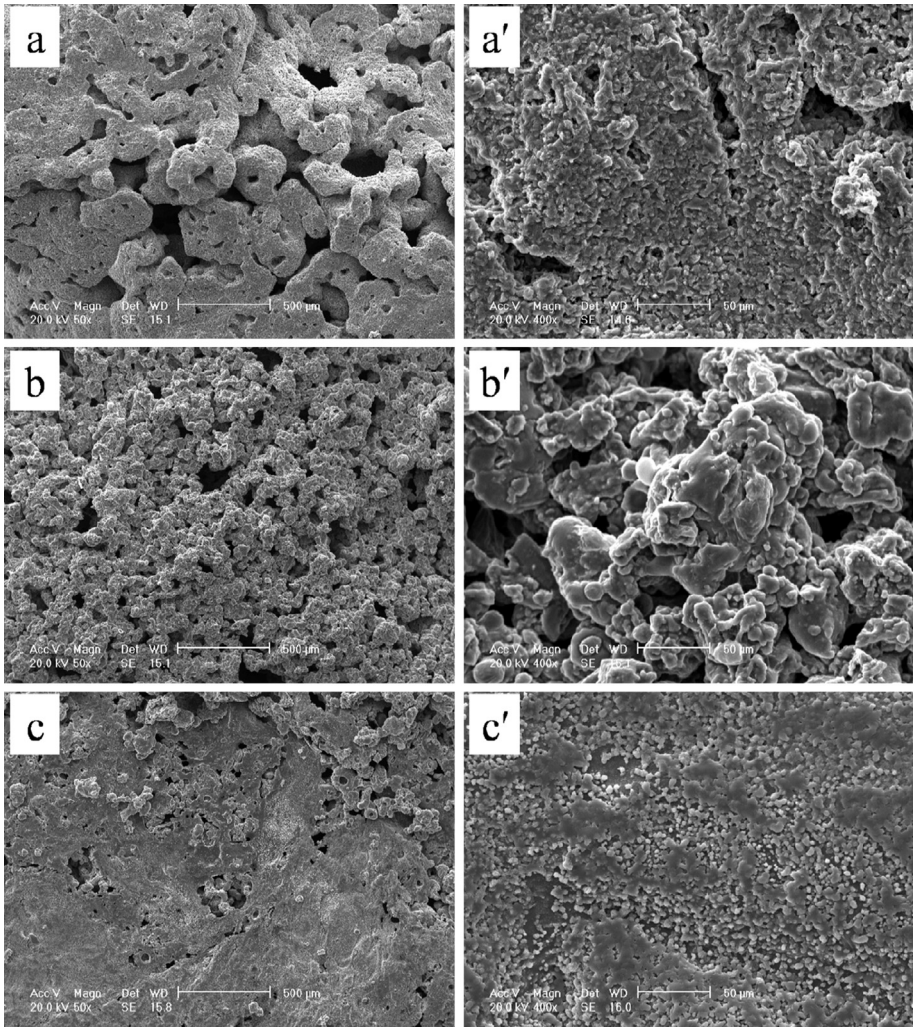

Fig. 10. SEM micrographs of the char residue formed after combustion: PBS/MP (a 50×, a′ 400×); PBS/MPi (b 50×, b′ 400×); PBS/MHP (c 50×, c′ 400×).

exist on the surface of char, which could be explained by the strong dehydration and catalytic carbonization effect of polyphosphates released from MP and the release of gas products from the composites, respectively. Fluffy and porous char residue can be observed from the SEM image (Fig. 10 (b and b′)) of PBS/MPi. The surface of PBS/MHP char residue (Fig. 10 (c and c′)) is more compact and smooth than those of PBS/MPi and MP, which can be attributed to catalytic carbonization of the phosphoric acid, which is produced from the reaction between PH_3 (largely generated from the decomposition of MHP) and oxygen covering the surface of materials.

3.7. Possible flame-retardant mechanism

Based on the detailed analysis above, it can be easily seen that the flame retarded efficiency and mechanism of MP, MPi and MHP in PBS matrix are different. The mechanism of MP in PBS composite is similar to the intumescent flame-retardant mechanism. MP acts as acid source and gas source, promoting the formation of intumescent char layer on the surface of PBS matrix during the combustion process. The intumescent char layer can hinder the propagation of oxygen and heat into the interior substrate, thus preventing the underlying materials from further burning. In addition, the inert volatile products (CO_2, NH_3) are beneficial to diluting the oxygen and flammable gas during burning in the gas phase. For MPi and MHP, except for the mechanism which is similar to that of MP, the release of PH_3 exerts special function. The generated PH_3 can be quickly oxidized to form H_3PO_4; then the phosphoric acid would further generate polyphosphoric acid to cover the surface of burning material and catalyze the formation of carbonaceous layer to avoid the fire [33,34]. Although the amount of PH_3 release in PBS/MHP is more than that of PBS/MPi, the flame retardant efficiency of the latter is higher than the former. This can be explained by that the temperature range of released PH_3 from MPi match better with the decomposition temperature of PBS. Therefore, the sequence of flame retardant efficiency in PBS matrix follows: MP < MHP < MPi.

4. Conclusions

This report presented the results of an investigation of the influence of phosphorus valence on flammability and thermal degradation of flame retarded poly(butylene succinate) composites. A series of PBS-based samples containing different amount of MP, MPi and MHP were prepared, which possessed different P oxidation state of +5, +3, and +1, respectively. The results obtained from LOI results indicated that the flame retarded efficiency of these three compounds in PBS matrix follows the sequence of MPi > MHP > MP at the same loadings. Meanwhile, the PHRR of PBS composites were significantly reduced compared with that of

pure PBS. The fire safety performance with the sequence of PBS/MPi > PBS/MHP > PBS/MP can also be obtained from the cone results. From the detailed analysis in gaseous phase and condensed phase by TG-IR and in situ FTIR, a conclusion can be drawn that except for the flame retarded action in gas phase through diluting the combustible gas by the release of non-flammable gases (CO_2, NH_3, etc.) from melamine structure in MP, MPi and MHP, a combined gas and solid phase action occurred in both MHP and MPi while only solid phase action has been revealed in MP. The decomposition of flame retardant matching with the decomposition temperature range of neat polymer is also an important factor. Therefore, the flame retarded efficiency of MPi was higher than that of MHP.

Acknowledgments

The work was financially supported by National Key Technology R&D Program (2013BAJ01B05), China Postdoctoral Science Foundation (2012M521246) and National Natural Science Foundation of China (51323010).

References

[1] Braun U, Schartel B. Flame retardant mechanisms of red phosphorus and magnesium hydroxide in high impact polystyrene. Macromol Chem Phys 2004;205:2185–96.
[2] Zhang S, Horrocks AR. A review of flame retardant polypropylene fibers. Prog Polym Sci 2003;28:1517–38.
[3] Braun U, Schartel B, Fichera MA, Jager C. Flame retardancy mechanisms of aluminium phosphinate in combination with melamine polyphosphate and zinc borate in glass-fibre reinforced polyamide 6,6. Polym Degrad Stabil 2007;92:1528–45.
[4] Brehme S, Schartel B, Goebbels J, Fischer O, Pospiech D, Bykov Y, et al. Phosphorus polyester versus aluminium phosphinate in poly(butylene terephthalate) (PBT): flame retardancy performance and mechanisms. Polym Degrad Stabil 2011;96:875–84.
[5] Tai QL, Song L, Hu Y, Yuen RKK, Feng H, Tao YJ. Novel styrene polymers functionalized with phosphorus-nitrogen containing molecules: synthesis and properties. Mater Chem Phys 2012;134:163–9.
[6] Swoboda B, Buonomo S, Leroy E, Cuesta JML. Fire retardant poly (ethylene terephthalate)/polycarbonate/triphenyl phosphite blends. Polym Degrad Stabil 2008;93:910–7.
[7] Bourbigot S, Duquesne S. Fire retardant polymers: recent developments and opportunities. J Mater Chem 2007;17:2283–300.
[8] Lv P, Wang ZZ, Hu KL, Fan WC. Flammability and thermal degradation of flame retarded polypropylene composites containing melamine phosphate and pentaerythritol derivatives. Polym Degrad Stabil 2005;90:523–34.
[9] Li QF, Li B, Zhang SQ, Lin M. Investigation on effects of aluminum and magnesium hypophosphites on flame retardancy and thermal degradation of polyamide 6. J Appl Polym Sci 2012;125:1782–9.
[10] Perret B, Schartel B, Stoss K, Ciesielski M, Diederichs J, Doring M, et al. Novel DOPO-based flame retardants in high-performance carbon fibre epoxy composites for aviation. Eur Polym J 2011;47:1081–9.
[11] Wang X, Hu Y, Song L, Xing WY, Lu HD, Lv P, et al. Flame retardancy and thermal degradation mechanism of epoxy resin composites based on a DOPO substituted organophosphorus oligomer. Polymer 2010;51:2435–45.
[12] Gu JW, Zhang GC, Dong SL, Zhang QY, Kong J. Study on preparation and fire-retardant mechanism analysis of intumescent flame-retardant coatings. Surf Coat Tech 2007;201:7835–41.
[13] Bourbigot S, Le Bras M, Duquesne S, Rochery M. Recent advances for intumescent polymers. Macromol Mater Eng 2004;289:499–511.
[14] Yang W, Hu Y, Tai QL, Lu HD, Song L, Yuen RKK. Fire and mechanical performance of nanoclay reinforced glass-fiber/PBT composites containing aluminum hypophosphite particles. Compos Part a-Appl S 2011;42:794–800.
[15] Zhao B, Chen L, Long JW, Chen HB, Wang YZ. Aluminum hypophosphite versus alkyl-substituted phosphinate in polyamide 6: flame retardance, thermal degradation, and pyrolysis behavior. Ind Eng Chem Res 2013;52:2875–86.
[16] Tang G, Wang X, Zhang R, Wang BB, Hong NN, Hu Y, et al. Effect of rare earth hypophosphite salts on the fire performance of biobased polylactide composites. Ind Eng Chem Res 2013;52:7362–72.
[17] Yao XL, Xie S, Chen CH, Wang QS, Sun JH, Li YL, et al. Comparative study of trimethyl phosphite and trimethyl phosphate as electrolyte additives in lithium ion batteries. J Power Sources 2005;144:170–5.
[18] Castrovinci A, Camino G, Drevelle C, Duquesne S, Magniez C, Vouters M. Ammonium polyphosphate-aluminum trihydroxide antagonism in fire retarded butadiene-styrene block copolymer. Eur Polym J 2005;41:2023–33.
[19] Thirumal M, Khastgir D, Nando GB, Naik YP, Singha NK. Halogen-free flame retardant PUF: effect of melamine compounds on mechanical, thermal and flame retardant properties. Polym Degrad Stabil 2010;95:1138–45.
[20] Jahromi S, Gabrielse W, Braam A. Effect of melamine polyphosphate on thermal degradation of polyamides: a combined X-ray diffraction and solid-state NMR study. Polymer 2003;44:25–37.
[21] Braun U, Balabanovich AI, Schartel B, Knoll U, Artner J, Ciesielski M, et al. Influence of the oxidation state of phosphorus on the decomposition and fire behaviour of flame-retarded epoxy resin composites. Polymer 2006;47:8495–508.
[22] Lorenzetti A, Modesti M, Besco S, Hrelja D, Donadi S. Influence of phosphorus valency on thermal behaviour of flame retarded polyurethane foams. Polym Degrad Stabil 2011;96:1455–61.
[23] Mariappan T, You Z, Hao JW, Wilkie CA. Influence of oxidation state of phosphorus on the thermal and flammability of polyurea and epoxy resin. Eur Polym J 2013;49:3171–80.
[24] Chen YJ, Zhan J, Zhang P, Nie SB, Lu HD, Song L, et al. Preparation of intumescent flame retardant poly(butylene succinate) using fumed silica as synergistic agent. Ind Eng Chem Res 2010;49:8200–8.
[25] Wang X, Song L, Yang HY, Lu HD, Hu Y. Synergistic effect of graphene on antidripping and fire resistance of intumescent flame retardant poly(butylene succinate) composites. Ind Eng Chem 2011;50:5376–83.
[26] Wang ZZ, Lv P, Hu Y, Hu KL. Thermal degradation study of intumescent flame retardants by TG and FTIR: melamine phosphate and its mixture with pentaerythritol. J Anal Appl Pyrol 2009;86:207–14.
[27] Chen YH, Wang Q. Reaction of melamine phosphate with pentaerythritol and its products for flame retardation of polypropylene. Polym Adv Technol 2007;18:587–600.
[28] Fernandez S, Mesa JL, Pizarro JL, Lezama L, Arriortua MI, Rojo T. Two new three-dimensional vanadium (III) and iron (III) phosphites templated by ethylenediamine: (C2H10N2)(0.5)[M(HPO3)(2)](center dot) ab initio structure determination, spectroscopic, and magnetic properties. Chem Mater 2002;14:2300–7.
[29] Schartel B, Hull TR. Development of fire-retarded materials – interpretation of cone calorimeter data. Fire Mater 2007;31:327–54.
[30] Chen XL, Huo LL, Jiao CM, Li SX. TG-FTIR characterization of volatile compounds from flame retardant polyurethane foams materials. J Anal Appl Pyrol 2013;100:186–91.
[31] http://webbook.nist.gov/chemistry [accessed December 2010].
[32] Ichikawa Y, Kondo H, Igarashi Y, Noguchi K, Okuyama K, Washiyama J. Crystal structures of alpha and beta forms of poly (tetramethylene succinate). Polymer 2000;41:4719–27.
[33] Jian RK, Chen L, Zhao B, Yan YW, Li XF, Wang YZ. Acrylonitrile-butadiene-styrene terpolymer with metal hypophosphites: flame retardance and mechanism research. Ind Eng Chem Res 2014;53:2299–307.
[34] Yan YW, Huang JQ, Guan YH, Shang K, Jian RK, Wang YZ. Flame retardance and thermal degradation mechanism of polystyrene modified with aluminum hypophosphite. Polym Degrad Stabil 2014;99:35–42.